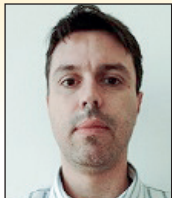


# Applications of a LITS semi-empirical model in plain and reinforced concrete members subjected to a uniaxial compressive load

## *Aplicações de um modelo semiempírico para o cálculo da fluência transiente em estruturas de concreto simples e armado submetidas a uma força de compressão centrada*



T. E. T. BUTTIGNOL <sup>a</sup>  
buttignol@hotmail.com

### Abstract

This paper describes a LITS (Load Induced Thermal Strain) semi empirical model and two practical applications in simple and reinforced concrete members. The model allows a preliminary and straightforward quantification of the total strain of concrete structures submitted to heating and a sustained compressive load, without the need to use complex numerical analyses. The model takes into account the effect of the thermal expansion restraint due to the boundary conditions (temperature and compressive load) and can be adopted for several types of concretes (conventional, high strength and ultra high performance). In the first example, the total deformations of simple concrete specimens from KHOURY (2006) are determined. In the second example, the total displacement of a reinforced concrete column from SCHNEIDER et al (1994) is calculated. A comparison between the results of the model and the experimental values demonstrated the reliability of the semi-empirical model to obtain a preliminary quantification of the total deformations of concrete.

**Keywords:** high temperature, transient creep, concrete, design procedures.

### Resumo

Este artigo descreve um modelo semiempírico para o cálculo da fluência transiente em concretos simples e armado submetidos a uma força de compressão durante o aquecimento, baseado no conceito de LITS (Load Induced Thermal Strain) ou deformação térmica induzida pelo carregamento. A partir do modelo, é possível a quantificação preliminar da deformação específica total do concreto submetido à alta temperatura sem a necessidade de utilização de complexas análises numéricas. O modelo leva em consideração o efeito de restrição da expansão térmica devido às condições de contorno (temperatura e força de compressão) e pode ser aplicado a diversos tipos de concreto, do convencional ao de alta resistência e ultra-alto desempenho. Dois exemplos práticos de aplicação são apresentados. No primeiro caso, é determinada a deformação específica total de corpos-de-prova em concreto simples previamente analisados por KHOURY (2006). No segundo exemplo é calculado o deslocamento total de um pilar em concreto armado investigado por SCHNEIDER ET AL (1994). A comparação dos resultados com os valores experimentais demonstraram a viabilidade do modelo para a determinação preliminar da deformação específica total de estruturas de concreto submetidas a uma força de compressão constante durante o incêndio.

**Palavras-chave:** alta temperatura, fluência transiente, concreto, técnicas de projeto.

<sup>a</sup> Universidade Presbiteriana Mackenzie, Campinas, SP, Brasil;  
<sup>a</sup> Universidade de São Paulo, Escola Politécnica, São Paulo, SP, Brasil.

## 1. Introduction and justification

One of the main problems of transient creep analysis is the fact that the viscous behavior cannot be measured directly from experimental tests in the laboratory. This is due the fact that transient creep is coupled with thermal (expansion and shrinkage) and mechanical (recoverable and irrecoverable) strains. In EUROCODE 2 (2004) transient creep is implicitly taken into account. It can be determined indirectly, for example, by means of LITS (Load Induced Thermal Strain), as described in Khoury (KHOURY et al., 1984; KHOURY et al., 1985; KHOURY, 2006a; KHOURY, 2006b). LITS is computed by the difference between the total strain, measured in loaded specimens, and the thermal strain, measured in unloaded specimens, subtracting the initial elastic deformation at 20°C. LITS concept was adopted in BUTTIGNOL (2016) to determine a new LITS semi-empirical model. In this paper, two practical applications of the semi-empirical model in concrete members subjected to a sustained uniaxial compressive load are presented.

It is important to underline that the principle of superposition is not always valid for concrete structures submitted to both a sustained compressive load and high temperatures. In this case, the sum of the thermal and mechanical strain components, obtained from independent numerical analyzes, could lead to completely different results from the total deformation measured in experimental tests. In the 1970's, ANDENBERG e THELANDERSSON (1976) performed an extensive experimental campaign with plain concrete specimens at high temperature. The authors demonstrated that the value of the total deformation of a previously loaded specimen is different from a specimen loaded immediately after heating. This difference can be attributed mainly to the effect of the boundary conditions: thermal expansion restraint imposed by the applied compressive load during heating.

A numerical analysis can be performed applying the boundary conditions and concrete thermomechanical properties in a mesoscopic level in order to correctly take into account the thermal effects and the loading conditions. Alternatively, empirical models, assuming implicitly the boundary conditions, can be applied. Different empirical models, proposed by distinct researchers, can be found in literature (TERRO, 1998; SCHNEIDER, 1986; TAO et al, 2013; ANDENBERG and THELANDERSSON, 1976). However, the models are calibrated considering a relatively small variety of concrete types, thus, limiting the range of their applications.

The great advantage of the LITS semi-empirical model (BUTTIGNOL, 2016) is the fact that it can be adopted for different types of concrete (conventional, high and ultra-high performance) to obtain a straightforward and preliminary quantification of concrete total deformation in concrete members submitted to high temperatures. The model can be an auxiliary tool to support design engineers in the evaluation of concrete deformations in a fire scenario.

## 2. Conceptual framework of transient creep

At room temperature creep occurs in concrete members submitted to a sustained load. It is the result of concrete relaxation (break and restoration of the links in the microstructure of the cement

paste). The continuous break and restoration of calcium-silicate-hydrates (CSH) due to fluid transport mechanisms (moisture diffusion) lead to concrete microprestress relaxation and, as a result, to an increase in the total deformation. Up to approximately 80°C, no changes in creep fundamentals are noticed, although, at this temperature level, creep value is twice the one observed at 20°C. At 100°C, all the free water the concrete is evaporated and the main mechanism of creep activation is due to concrete dehydration (CSH physical and chemical water loss). At this stage, concrete viscous deformation during heating is usually defined as transient creep. Beyond 400°C, an acceleration of transient creep (increase of deformation) occurs due to the progressive degradation of the coarse aggregates.

Transient creep is quasi-instantaneous, since CSH dehydration (chemical bond breakages and water evaporation) occurs due to the effect of high temperatures in the cement paste. Immediately after heating, when the temperature stabilizes, transient creep continues to develop due to thermal differentials.

According to SABEUR et al. (2008), up to 400°C, concrete dehydration is the main mechanism of activation of transient creep.

TAO et al. (2013) sustain that the two most important mechanisms of transient creep activation are the CSH dehydration and portlandite decomposition.

SABEUR and MEFTAH (2008) distinguish transient creep in two components: drying creep, due to free water evaporation at approximately 100°C, and dehydration creep, due to CSH physical and chemical water loss.

MINDEGUIA et al. (2006) measured concrete radial displacements, concluding that transient creep virtually is not activated in this direction.

GILLEN (1981) states that transient creep is highly affected by water/cement (w/c) ratio at temperatures around 110°C.

According to KHOURY (2006b), LITS is absent in concrete structures during a second heating cycle, up to the maximum temperature achieved in the first cycle.

MINDEGUIA et al. (2013) support that in concrete members submitted to a previous heating, transient creep appears only at temperatures higher than those reached by the preheated specimen.

KHOURY (2006a) affirms that LITS is developed at the cement paste level and, thus, it is insensitive to the aggregate type up to 450°C. Moreover, concrete thermal stability depends specifically on the type of aggregate. In agreement with that, MINDEGUIA et al. (2013) state that transient creep is influenced by the nature of the aggregates at temperatures beyond 300°C.

During the cooling phase, no significant sign of transient creep or shrinkage was observed by KHOURY (2006b). The action of the compressive load restrained cracking propagation and other expansive deformations.

SABEUR and COLINA (2014) observed the separation of the cement paste from the aggregates during cooling due to the effect of microcracking. This result was attributed to the absence of transient creep during cooling.

According to SABEUR and COLINA (2014), transient creep is inversely proportional to the w/c ratio, which is directly related to concrete permeability.

In the experimental tests carried out by SABEUR and COLINA (2014), up to 220°C, the smallest values of transient creep were

measured in conventional concrete, followed by high-strength concrete and high-performance concrete.

The incorporation of polypropylene (PP) fibers (WU et al, 2010; HUISMANN et al., 2012; e TAO et al., 2013) increases transient creep due to microcracking effect (increase of concrete porosity due to fibers melting).

### 3. Description of the LITS semi-empirical model (BUTTIGNOL, 2016)

The semi-empirical model recognizes concrete as a heterogeneous biphasic material (aggregates + matrix) and defines LITS as the sum of thermomechanical and thermochemical strains. The former is developed in the bulk concrete (aggregates and cement paste) and it is the result of microcracking, aggregates degradation and thermal expansion restraint imposed by the compressive load. Microcracking occurs due to thermal mismatch (aggregates expansion and cement paste shrinkage) beyond 150°C. The coarse aggregates are responsible for LITS acceleration after 400°C due to chemical transformations (especially quartz  $\alpha$ - $\beta$  phase transformation at 573°C), fracture and decomposition of the material. The thermochemical strain is seated in the cement paste and, thus, it is insensitive to the type of aggregate. Its main mechanisms of activation are the free water evaporation (drying creep) around 100°C and CSH physical and chemical water loss (dehydration creep) beyond 150°C.

Drying creep is highly affected by hygrothermal conditions before heating. A concrete submitted to thermal curing exhibits no drying creep. Dehydration creep is the main mechanism of transient creep up to 400°C, from which point, the behavior of the aggregates becomes increasingly important.

The semi-empirical model is defined in terms of specific LITS (1/MPa) or  $J_{LITS}(\theta)$ , as shown in Equation 1, where:  $q_{tm}(\theta)$  is the thermomechanical function for siliceous, calcareous and basalt aggregate type, in 10<sup>3</sup>/MPa (Equation 2);  $q_{tc}(\theta)$  is the thermochemical function in 10<sup>-3</sup>/MPa (Equation 3);  $\beta_{tm}$  is the variable dependent on the quantity of aggregates (c.agg.) and binder (Equation 4);  $\beta_{tc}$  is the variable dependent on the quantity of binder (equation 5). The temperature is given in °C. The quantities of aggregates and binder are given in kg.

$$J_{LITS}(\theta) = \beta_{tm} \times q_{tm}(\theta) + \beta_{tc} \times q_{tc}(\theta) \quad (1)$$

$$q_{tm}(\theta) = (-5.26 \times 10^{-5} \times \theta - 9.73 \times 10^{-7} \times \theta^2 + 3.23 \times 10^{-9} \times \theta^3 - 4.42 \times 10^{-12} \times \theta^4) \quad (2)$$

$$q_{tc}(\theta) = -\exp(\theta^{0.31}) \times 0.156^5 \quad (3)$$

$$\beta_{tm} = \ln\left(1 + \left(\frac{cagg}{binder}\right)^3\right) \quad (4)$$

$$\beta_{tc} = \ln\left(\frac{binder}{100}\right) \quad (5)$$

Total LITS (in mm/m) is calculated according to Equation 6 and LITS coefficient ( $\phi_{LITS}$ ) is determined according to Equation 7, where:  $\sigma$  is the compressive stress level ( $P/A$ ) in MPa;  $E_{ci}$  is the initial tangent modulus of elasticity.

$$LITS = J_{LITS}(\theta) \times \sigma \quad (6)$$

$$\phi_{LITS} = J_{LITS}(\theta) \times E_{ci} \quad (7)$$

It is important to mention that recycled aggregates are decomposed approximately at 400°C, while siliceous and calcareous aggregates are stable up to 1200°C. In order to take into account the behavior of the different aggregate types (calcareous, siliceous, basalt, recycled), two thermomechanical functions were derived. The thermomechanical function for recycled aggregates is described in Equation 8 and for the other types of aggregates is shown in Equation 2.

$$q_{tm,recycled}(\theta) = (-3.5 \times 10^{-7} \times \theta^2 + 1.7 \times 10^{-9} \times \theta^3 - 1.3 \times 10^{-11} \times \theta^4 + 2.4 \times 10^{-14} \times \theta^5) \quad (8)$$

### 4. Practical applications of the semi-empirical model

In this section, two practical examples of application of the semi-empirical model are analyzed. In the first case, KHOURY (2006) experimental results of plain concrete specimens, considering a heating rate of 1 °C/min and a maximum temperature of 600°C, are compared with the semi-empirical model (BUTTIGNOL, 2016). In this case, due to the low heating rate, a small thermal gradient is developed in the bulk concrete. Hence, concrete total deformation can be defined as the sum of LITS, the thermal strain and the initial elastic strain at 20°C, as is shown in Equation 10.

In the second example, the total displacement of a reinforced concrete (RC) column under fire, previously analyzed in SCHNEIDER (1994), is calculated. In this case, it is not possible to apply directly the semi-empirical model due to concrete thermal differentials (self-equilibrated stresses) and the compatibility between concrete and steel bars deformation (transient creep effects in concrete are absent in steel). As a result, the semi-empirical model was incorporated in a numerical model to find the solution, as is described below.

#### 4.1 Numerical model

Concrete total deformation under a fire scenario can be defined in terms of LITS, as is shown in Equations 9 and 10, where:  $\varepsilon^t$  is the total deformation;  $\varepsilon^{th}$  is the thermal strain;  $\varepsilon_{ci}(\theta = 20^\circ \text{C})$  is the initial elastic strain at room temperature.

$$LITS = \varepsilon^t - \varepsilon^{th} - \varepsilon^{el}(\theta = 20^\circ \text{C}) \quad (9)$$

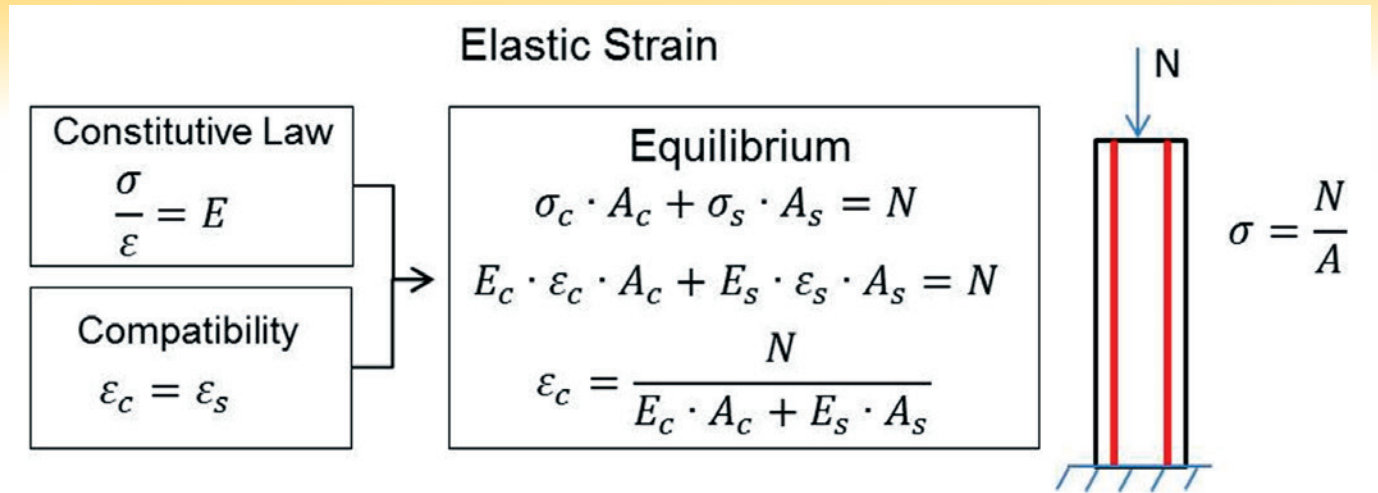


Figure 1 Compatibility between concrete and steel bars deformation

$$\varepsilon^t = LITS + \varepsilon^{th} + \varepsilon^{el} \quad (\theta = 20^\circ C) \quad (10)$$

Concrete and steel plastic strains (irrecoverable deformation) are not taken into account in the analyses carried out in this paper, despite the recognition of their importance and effects to concrete

total deformation. They can be included in numerical models by properly defining the materials thermomechanical properties and a damage model that takes into account concrete physical-chemical transformations at high temperatures. This is out of the scope of this paper.

In the first case, the specimens are submitted to a low heating

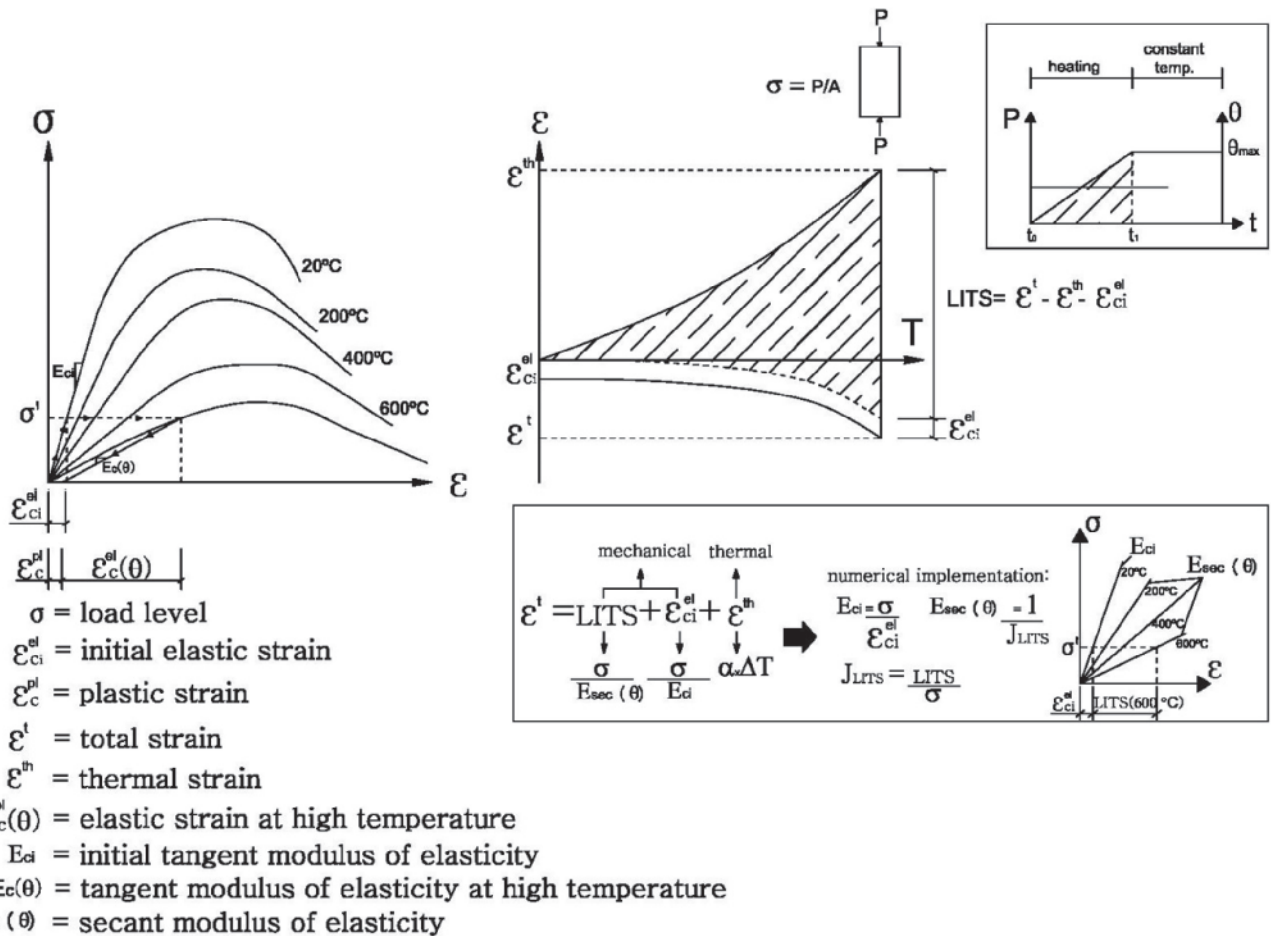


Figure 2 Fictitious linear-elastic model (secant modulus of elasticity) adopted in the finite element software Abaqus 2D

**Table 1**  
Concrete mix design ( $\text{kg}/\text{m}^3$ ) (Khoury, 2006)

Cement	Fine agregastes	Coarse agregastes	Water
415	750	1120	187

rate ( $1^\circ\text{C}/\text{min}$ ), which generates self-equilibrated stresses of small magnitude. Besides, a maximum compressive load of  $0,20f_c$  is applied, together with a maximum temperature of  $600^\circ\text{C}$ , which keep the specimen mainly in a viscoelastic regime.

In the second case, a RC column is submitted to a standard fire curve (Equation 11), inducing relatively high values of self-equilibrated stresses. Moreover, concrete sections close to the borders are exposed to very high temperatures ( $\theta > 1000^\circ\text{C}$ ), which lead to high plastic deformations. Hence, further and more rigorous analyzes should be carried out to have a better approximation of the results. The compatibility between concrete and steel bars deformation is shown in Figure 1.

The steel bars, although subjected to thermal creep, do not manifest transient creep. The latter is characterized by the quasi-instantaneous deformation that occurs in concrete members subjected to a sustained compressive load during heating. The increase of temperature leads to free water evaporation (drying creep) and CSH dehydration (microstress relaxation in the nanostructure of the cement paste).

The finite element software Abaqus 2D was used to calculate the total displacement of the RC column. In order to do so, a fictitious linear-elastic model incorporating LITS semi-empirical model was adopted, as is described in Figure 2. The initial modulus of elasticity was determined from the elastic strain at  $20^\circ\text{C}$  ( $E_{ci} = \sigma / \epsilon_{ci}^{el}$ ). The secant modulus of elasticity is dependent of the temperature and was determined from the specific LITS (semi-empirical model):  $E_{sec}(\theta) = 1 / J_{LITS}$ .

The same approach (numerical model) was adopted to calculate the total deformation of plain concrete specimens from KHOURY

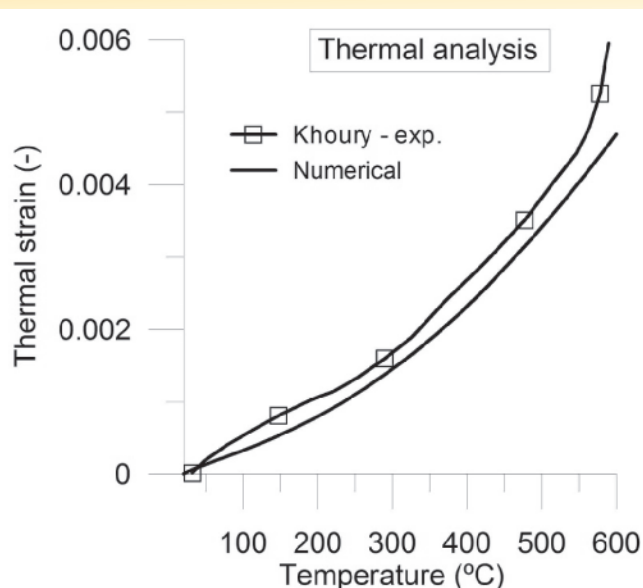


**Figure 3**

Comparison between numerical and experimental thermal strain values

(2006). The numerical results were compared both with the experimental values and the ones obtained from Equation 10, applying directly the semi-empirical model (Equation 6).

#### 4.2 Total deformation of plain concrete specimens

The total deformation of plain concrete specimens with  $75\text{ mm} \times 100\text{ mm}$ , submitted to a heating rate of  $1^\circ\text{C}/\text{min}$ , up to a maximum temperature of  $600^\circ\text{C}$ , is determined and compared with the experimental results obtained from KHOURY (2006). The specimens have a compressive strength of  $61\text{ MPa}$  and a modulus of elasticity equal to  $47\text{ GPa}$ .

Concrete mix design is shown in Table 1.

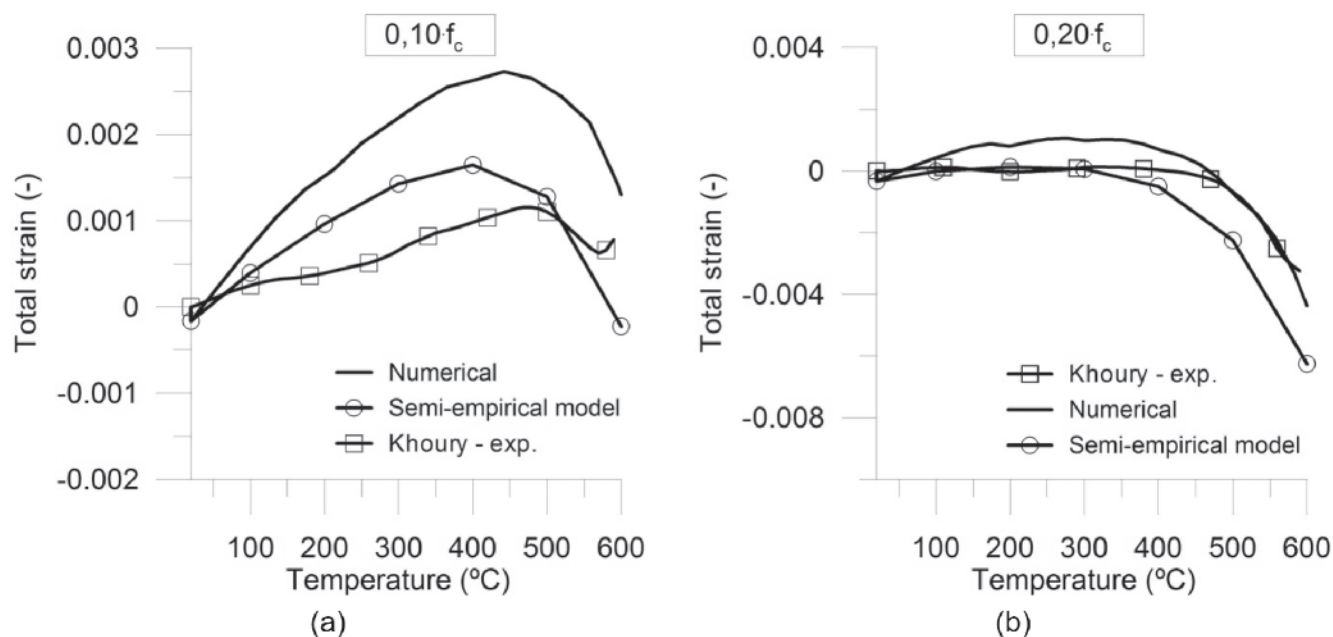


**Figure 4**

Comparison between the experimental values and the results obtained using the semi-empirical model for a load level respectively equal to: a)  $0,10f_c$ ; b)  $0,20f_c$

**Table 2**

Mechanical properties of the materials (Schneider, 1994)

	Concrete		Steel
$f_{ck}$	50 MPa	$f_{yk}$	375,9 MPa
$E_{ci}$	35 GPa	$E_s$	208 GPa

Concrete thermal strain was calculated using Abaqus 2D, assuming a coefficient of thermal expansion equal to  $1,0 \times 10^{-5} 1/^\circ C$ . A comparison between the numerical and experimental results is shown in Figure 3.

The total deformation was calculated both according to Equation 10, using the semi-empirical model (Equations 1 and 6) and by means of a numerical analysis, as described in subsection 4.1. The results, for a sustained load equal to a  $0,10f_c$  and  $0,20f_c$ , are shown in Figure 4, together with KHOURY (2006) experimental values.

The results demonstrate a good approximation between the experimental values and the ones obtained from the semi-empirical model. It is worth mentioning that LITS variation, as function of the load level, is not perfectly linear, as is assumed in the semi-empirical model. Besides, the variation between the values obtained from Equation 10 and from the numerical analysis is mainly due to the fact that the numerical model takes into account the thermal differentials inside the specimen, which is completely disregarded by the semi-empirical model. In this particular case, due to the low heating rate, this difference is small and does not have a significant influence in the results.

### 4.3 Total displacement of a RC column

The total displacement of a RC column subjected to a sustained compressive load and exposed to fire (SCHNEIDER, 1994) is computed using the semi-empirical model, according to the procedures described in subsection 4.1 (numerical analysis).

The column is reinforced with four steel bars with 16 mm diameter, concrete cover of 40 mm and stirrups of 6 mm diameter. The column cross-section is equal to 300 mm x 300 mm, with an effective height (area exposed to fire) of 1200 mm. The materials mechanical properties (Table 2), concrete mix design (Table 3) and the column characteristics (geometry and reinforced bars) were obtained from SCHNEIDER et al (1994).

The standard fire curve adopted by SCHNEIDER et al (1994), assuming an overall fire duration of 180 minutes, is shown in Equation 11, where:  $\theta$  is the temperature in  $^\circ C$ ;  $t$  is the time in minutes.

$$\theta = 460 \times t^{\frac{1}{6}} + 20 \tag{11}$$

**Table 3**

Concrete mix design ( $kg/m^3$ ) (Schneider, 1994)

Cement	Fine aggregates	Coarse aggregates	Water	Superplasticizers
500	673	1067	175	8,0

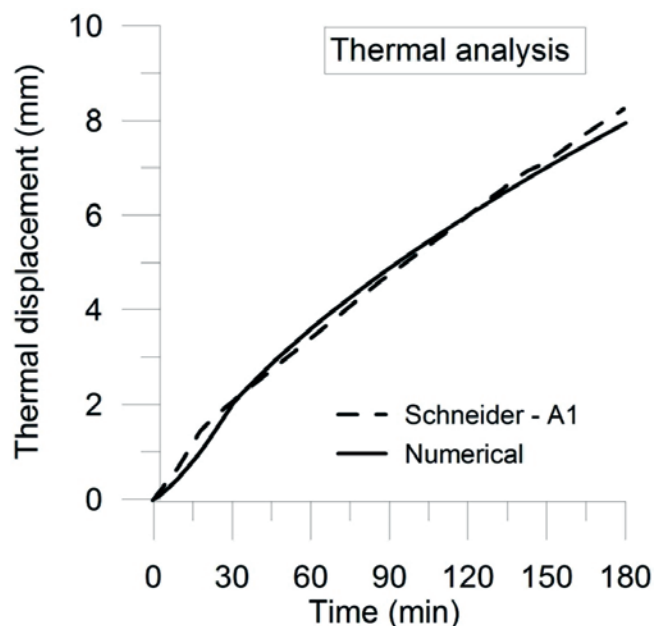


**Figure 5**  
Thermal displacement values of a RC column

The thermal strain ( $\epsilon^{th}$ ) was obtained by means of a numerical analysis carried out in Abaqus 2D. In this case, the same coefficient of thermal expansion ( $\alpha = 1,0 \times 10^{-5} 1/^\circ C$ ) was adopted both for concrete and steel. The comparison between the experimental (Schneider – A1) and numerical results is shown in Figure 5.

The total displacement was determined for two different load levels:  $0,15f_c$  e  $0,30f_c$ . The numerical results were compared with the experimental values (SCHNEIDER et al, 1994) in terms of displacement *versus* time as is shown in Figure 6. Two nominally identical tests for each load level were performed by SCHNEIDER et al (1994): “B1” and “B2” for a compressive load equal to  $0,15f_c$ ; “B3” and “B4” for a compressive load equal to  $0,30f_c$ .

From the results, one can observe a reasonable approximation between the experimental values and the ones obtained using the semi-empirical model. It is worth noting that the numerical model adopted in the analyzes completely neglects the plastic deformations developed during heating, which are mainly concentrated in the areas close to the external surface due to the high temperature level reached in these regions ( $\theta > 1000^\circ C$ ).

## 5. Conclusions

The main advantage of the model described in this paper (BUTTI-GNOL, 2016) is that it can be adopted for different types of

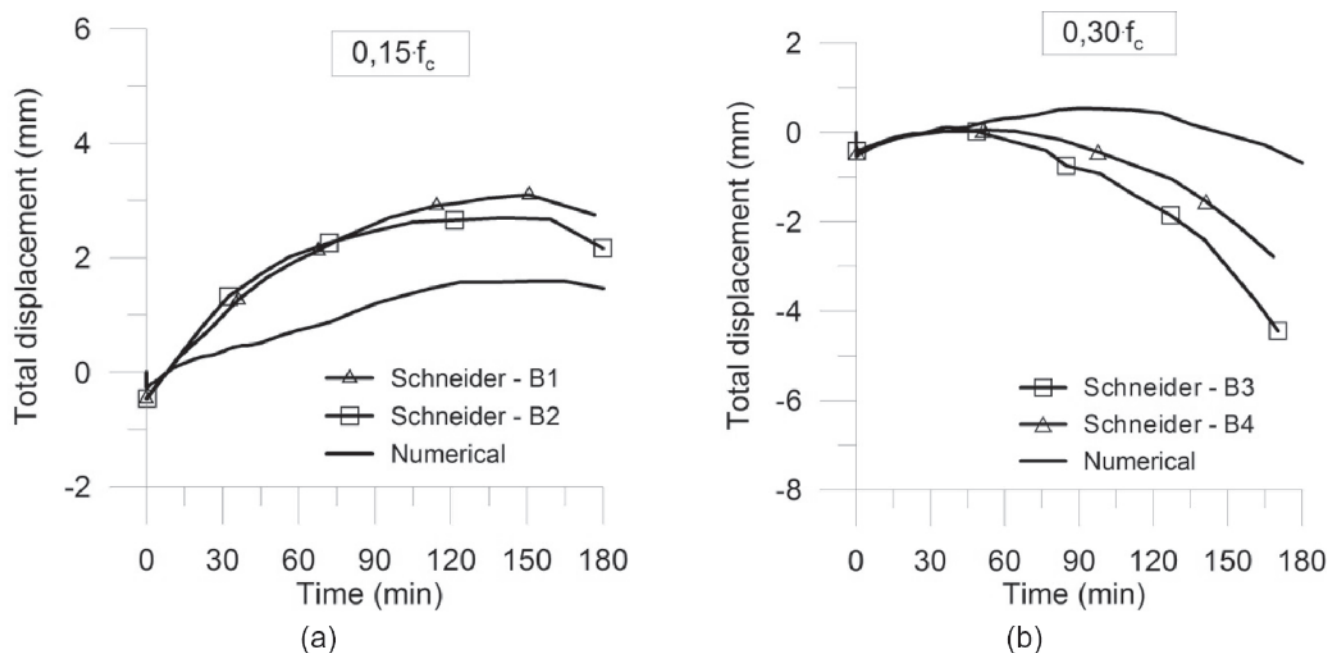


**Figure 6**  
Total displacements of a RC column considering a load level equal to: a)  $0,15f_c$ ; b)  $0,30f_c$

concrete (conventional, high and ultra-high performance) to perform a preliminary analysis of concrete members submitted to a fire scenario. The model allows a straightforward quantification of the total deformation without the need to recur to complex numerical models, based on the materials thermomechanical properties and the boundary conditions.

The semi-empirical model was applied to calculate the total deformation of plain concrete specimens from KHOURY (2006) and the total displacement of a RC column from SCHNEIDER et al (1994). The comparison between the experimental and semi-empirical model results demonstrated the reliability of the proposed model.

## 6. Acknowledgements

The author would like to acknowledge CNPq (Conselho Nacional de Desenvolvimento Científico e Tecnológico) for its financial support of this work through a PhD research scholarship.

## 7. Bibliography

- [1] EN 1992-1. Eurocode 2: Design of concrete structures. Part 1-2 - General rules - Structural Fire Design. British Standards, 2004.
- [2] ANDENBERG, Y. e THELANDERSSON, J.. Stress and deformation characteristics of concrete at high temperatures. Technical report, Lund Institute of Technology, 1976.
- [3] BUTTIGNOL, T. E. T. On the Load Induced Thermal Strain for Plain and Steel Fiber Reinforced Concrete Subjected to Uniaxial Loading. PhD thesis, Politecnico di Milano, 2016.
- [4] GILLEN, M.. Short-term Creep of Concrete at Elevated Temperatures. *Fire and Materials*, vol. 5, nº 4, pp. 142-148, 1981.
- [5] HUISMANN, S; WEISE, F.; MENG, B. e SCHNEIDER, U.. Transient strain of high strength concrete at elevated temperatures and the impact of polypropylene fibers. *Materials and Structures*, nº 45, pp. 793-801, 2012.
- [6] KHOURY, G. A.; SULLIVAN, P. J. E. e GRAINGER, B. N.. Radial temperature distributions within solid concrete cylinders under transient thermal states. *Magazine of Concrete Research*, vol. 36, pp. 146-156, 1984.
- [7] KHOURY, G. A.; GRAINGER, B. N. e SULLIVAN, P. J. E.. Strain of concrete during first heating to  $600^{\circ}\text{C}$  under load. *Magazine Concrete Research*, nº 37, pp. 195-215, 1985.
- [8] KHOURY, G. A.. Strain of heated concrete during two thermal cycles. Part 1: strain over two cycles, during first heating and at subsequent constant temperature. *Magazine of Concrete Research*, nº 6, pp. 367-385, 2006a.
- [9] KHOURY, G.. Strain of heated concrete during two thermal cycles. Part 3: isolation of strain components and strain model development. *Magazine of Concrete Research*, nº 7, pp. 421-435, 2006b.
- [10] MINDEGUIA, J.-C., PIMIENTA, P.; HAGER, I.; LA BORDERIE, B. e CARRE, H.. Experimental study of transient thermal strain and creep of an ordinary concrete at high temperatures. Fourth International Workshop - Structures in Fire, Aveiro, Portugal, 2006.
- [11] MINDEGUIA, J.-C.; HAGER, I.; PIMIENTA, P.; CARRÉ, H. e LA BORDERIE, C.. Parametrical study of transient thermal strain of ordinary and high performance concrete. *Cement and Concrete Research*, nº 48, pp. 40-52, 2013.

- [12] SABEUR, H e MEFTAH, F.. Dehydration creep of concrete at high temperatures. *Materials and Structures*, vol. n. 3, pp. 17-30, 2008.
- [13] SABEUR, H.; MEFTAH, F.; COLINA, H. e PLATRET, G.. Correlation between transient creep of concrete and its dehydration. *Magazine of Concrete Research*, n° 3, pp. 157-163, 2008.
- [14] SABEUR, H. e COLINA, H.. Effect of heating–cooling cycles on transient creep strain of high performance, high strength and ordinary concrete under service and accidental conditions. *Materials and Structures*, 2014.
- [15] SCHNEIDER, U; MORITA, T.; FRANSSEN, J-C. A Concrete Model Considering the Load History Applied to Centrally Loaded Columns Under Fire Attack. *Fire Safety Science – Proceedings of the 4th International Symposium*, pp. 1101-1112, 1994.
- [16] TAO, J.; LIU, X.; YUAN, Y. e TAERWE, L.. Transient strain of self-compacting concrete loaded in compression heated to 700°C. *Materials and Structures*, n° 46, pp. 191-201, 2013.
- [17] WU, B., et. al.. Creep Behavior of High-Strength Concrete with Polypropylene Fibers at Elevated Temperatures. *ACI Materials Journal*, March-April, pp. 176-184, 2010.